



RELATING POSITION UNCERTAINTY TO MAXIMUM CONJUNCTION PROBABILITY[©]

Salvatore Alfano



Copyright © 2003 by The Aerospace Corporation. Published by the American Astronautical Society, with permission

AAS/AIAA Astrodynamics Specialists Conference

Big Sky Resort, Big Sky, Montana, August 3-7, 2003

AAS Publications Office, P.O. Box 28130, San Diego, CA 92198

Relating Position Uncertainty to Maximum Conjunction Probability[©]

Salvatore Alfano*

This analysis shows the effects of positional uncertainty on the gaussian probability computation for orbit conjunction. Relative motion between two objects is assumed linear for a given encounter with time-invariant position covariance. A method is developed to map regions of maximum probability for various satellite sizes, encounter geometries, and covariance sizes and shapes. Those regions are then examined to assess probability dilution. The assertion is made that orbit positions should be sufficiently accurate to avoid these dilution regions. Charts are provided to assist the reader in determining orbital accuracy requirements that will prevent or minimize dilution of the probability calculations.

INTRODUCTION

Probability calculations for conjunction analysis of orbiting objects should ensure sufficient accuracy to give meaningful results. If the positional uncertainty is very large, a gaussian calculation will produce a low conjunction probability. Although mathematically correct, the resulting probability may give a false sense of confidence that a conjunction is not likely to occur. Such a low probability may, in fact, indicate that the data is not of sufficient accuracy to produce a meaningful result.

Much work has been done to address the computing of probability for neighboring space objects¹⁻⁹ and some work has been done to examine accuracy requirements¹⁰. Typically, one determines if and when a secondary object will transgress a user-defined safety zone. The uncertainties associated with position are represented by three-dimensional gaussian probability densities. These densities take the form of covariance matrices and can be obtained from the owner-operators or independent surveillance sources such as the US Satellite Catalog (Special Perturbations). Typically, positions and covariances are propagated to the time of closest approach, relative motion is assumed linear, and the positional covariances are assumed constant and uncorrelated for the encounter.

* Salvatore Alfano, Senior Project Engineer, The Aerospace Corporation
1150 Academy Park Loop, Suite 136, Colorado Springs, CO 80910
salvatore.alfano@aero.org 719-638-2299

A plane perpendicular to the relative velocity vector is formed and the objects and their covariances are projected onto this plane. This projection reduces the dimensionality of the problem from three to two by eliminating the element associated with time of conjunction. The covariances are assumed to be uncorrelated and are summed to form a **combined covariance centered on the secondary object**. The radii of the two objects are summed to form a combined, spherical **hard-body; its projection is circular and centered at the primary**.

Visually the covariances are combined to form one large ellipsoid centered about the secondary. The primary object passes through the combined covariance ellipsoid creating a tube-like path. This analysis compresses the dimension associated with the tube path (i.e. relative velocity) and the tube becomes a circle on the projected plane (also known as the collision plane). The secondary object also appears as a circle in the plane. The probability associated with the compressed dimension becomes unity, leaving only a two-dimensional probability calculation to be performed in the collision plane.

A conjunction occurs when the path (tube) of the primary object touches the secondary object. In the collision plane this happens when the distance between the two projected object centers is less than the sum of their radii. The probability of the **footprint** of a circle defining such a family of radii is then computed using the combined, projected covariance. This yields a cumulative (as opposed to instantaneous) probability.

METHODOLOGY

For all cases, the space platforms are assumed spherical with combined **object sizes varying from 1 meter to 40 meters**. The covariance ellipse aspect ratio is varied from 1 (spherical) to 100 (soda straw). **Miss distance is varied from 50 meters to 10 kilometers**. **The maximum probability for each case is determined by orienting and sizing the covariance matrix to achieve such**.

To assist the reader in interpreting the charts that follow, it is necessary to explain their construction. **For the initial case, a close approach distance (offset) of 1000 meters** is plotted for a spherical covariance ellipsoid. Figure 1 shows that for very small deviations, the offset causes the object to be many standard deviations from the covariance ellipse center. This results in very small values for probability. As the standard deviation increases the probability reaches a maximum. Continuing to increase the standard deviation causes the probability to decrease. As Figure 1 indicates, any standard deviation that is greater than the one that produces maximum probability causes a dilution in the probability computation. As expected, the greater the object size, the greater the footprint in the collision plane, and the greater the probability.

Probability with 1000m Offset

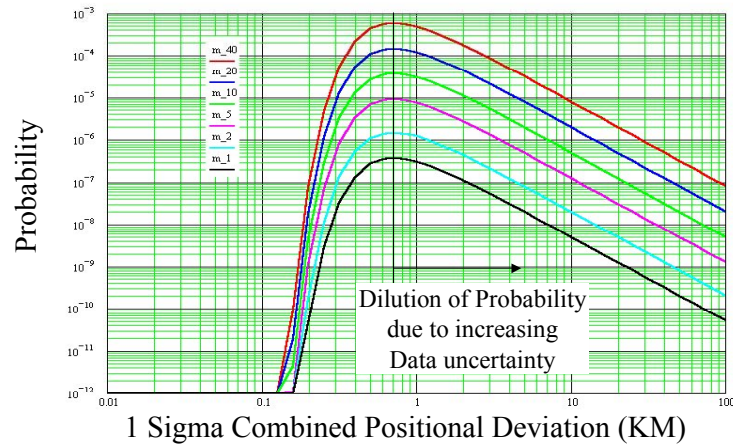


Fig. 1 Probability versus Deviation for 1000m Closest Approach Distance

The next step in this analysis is to produce a chart containing all the maximum probabilities for a family of offsets. To create such a chart, the previous assumptions are used but only the maximums are plotted. Only plots for offsets of 100, 500, and 100 meters are shown in Figure 2 for a combined object radius of 1 meter and one of 40 meters.

Maximum Probability Analysis (AR = 1)

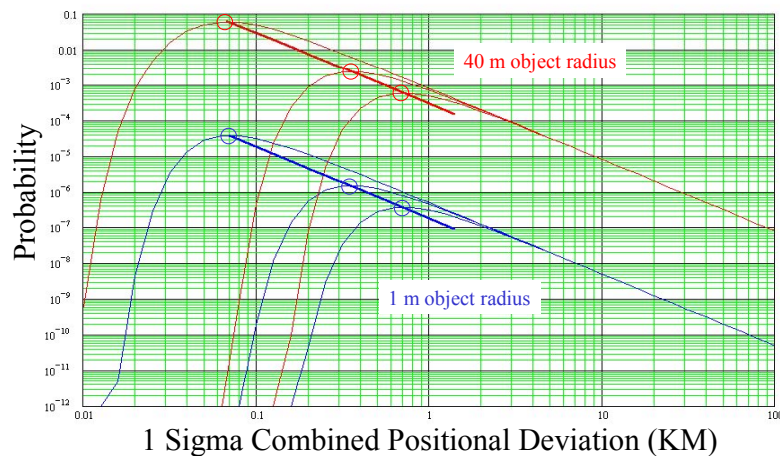


Fig. 2 Determining Regions of Maximum Probability

This is done to reduce clutter in this instructional figure. The maximums for all offsets and object sizes can be combined into one chart as represented in Figure 3.

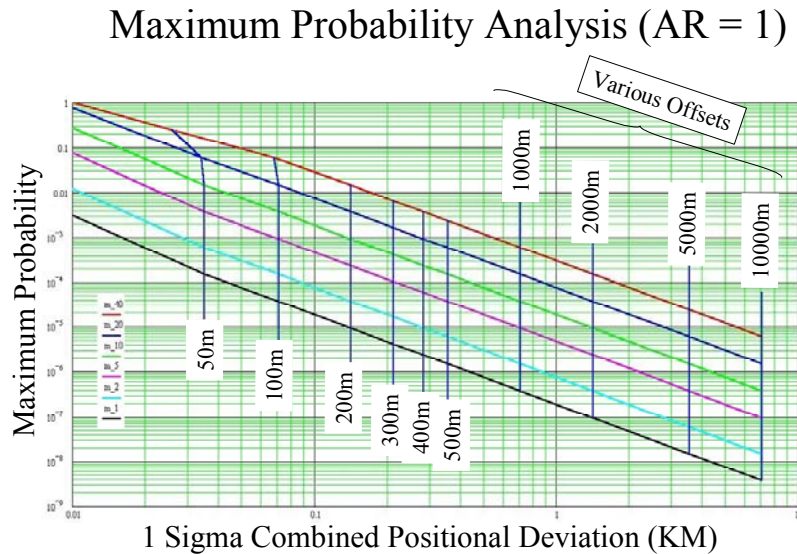
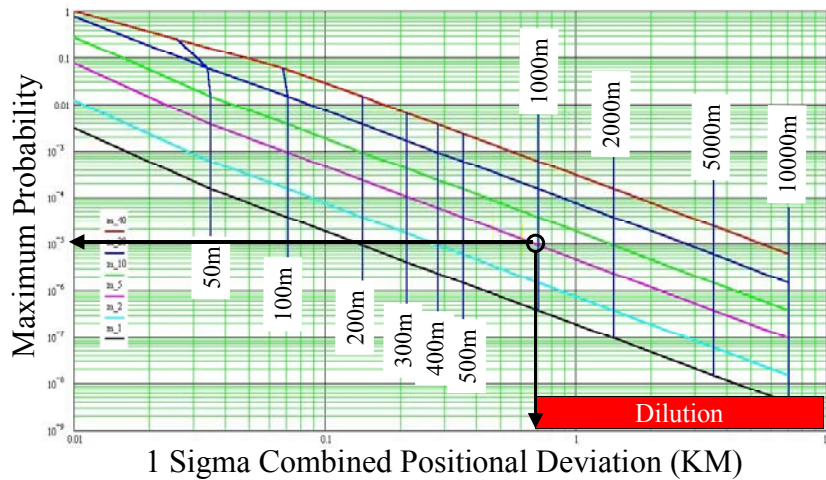


Fig. 3 Maximum Probability Analysis for Spherical Covariance

There are four pieces of information given in Figure 3: distance offset, maximum probability, combined positional deviation, and combined object radius. Given any two pieces of information, the chart can be used to determine the remaining two. As an example, consider two space objects 1000 meters apart and having a combined radius of 5 meters. From Figure 4 the maximum probability is shown to be 10^{-5} (ordinate value), meaning it is mathematically impossible to exceed this value for the stated assumptions. If an operator were to define a probability threshold of 10^{-4} for maneuvering to avoid a potential collision, then that operator could rest assured that no further action is necessary. Figure 4 also shows a combined positional deviation of 700 meters (abscissa value). Dilution occurs when the combined positional uncertainty (deviation) is greater than 700 meters. The ephemerides of the two conjuncting objects should have uncertainties that, when combined, do not exceed a standard deviation of 700 meters. If the uncertainties are greater, then dilution occurs and the operator may get a false sense of security from any subsequent probability calculation. In this manner, one can deduce minimum accuracy

requirements for meaningful probability

Maximum Probability Analysis (AR = 1)



analysis.

Fig. 4 Example to Determine Maximum Probability and Accuracy

Maximum Probability Analysis (AR = 1)

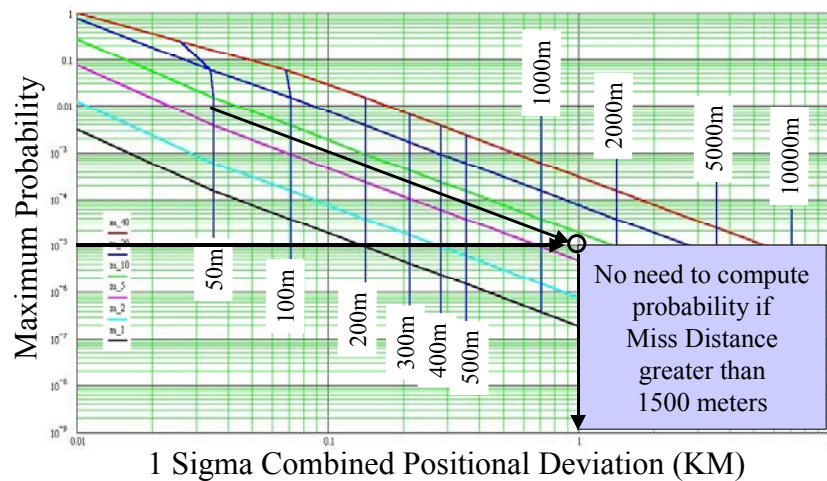


Fig. 5 Example to Determine Keepout Zone Distance

Figure 5 shows another example of chart use. A decision probability threshold of 10^{-5} is used for two objects with a combined radius of 8 meters. Interpolation is required because the chart does not explicitly show an 8 meter

radius. For undiluted probability analysis, a combined deviation of 1000 meters should not be exceeded. If the closest approach distance is greater than 1500 meters, then the probability threshold will never be exceeded. This shows how to determine keepout zone distances based on probability.

Thus far, the representation has only addressed the case where positional uncertainty in each axis is identical. The same approach can be applied to non-spherical covariance ellipsoids by building a chart for each ratio of maximum-to-minimum deviation in the collision plane. These aspect ratios (ARs) of major-to-minor axes add a degree of complexity because orientation in the plane alters the probability calculation. These analyses address dilution, so the projected covariance is always oriented to produce the maximum probability for a given distance offset. The abscissa in the subsequent figures is changed to reflect the deviation size of the covariance ellipse's major axis in the projected plane.

Figures 6 through 9 reflect the changes in maximum probability when the aspect ratio is varied from 1 to 100. The reader is reminded that the abscissa values represent the standard deviation of the combined covariance ellipse major axis, which is the square root of the sum of the square of the individual deviations. Returning to the example presented in Figure 4, 700 meters was determined to be the combined positional deviation to prevent dilution. Assuming the deviations were the same for both objects, the 1σ ephemeris accuracy at time of conjunction must be good to 495 meters (700 divided by the square root of 2).

Maximum Probability Analysis (AR = 3)

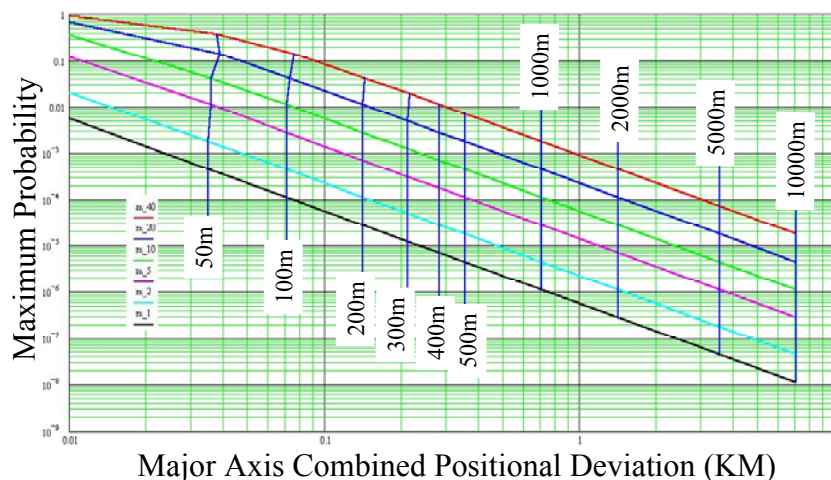


Fig. 6 Maximum Probability Chart for Aspect Ratio of 3

Maximum Probability Analysis (AR = 5)

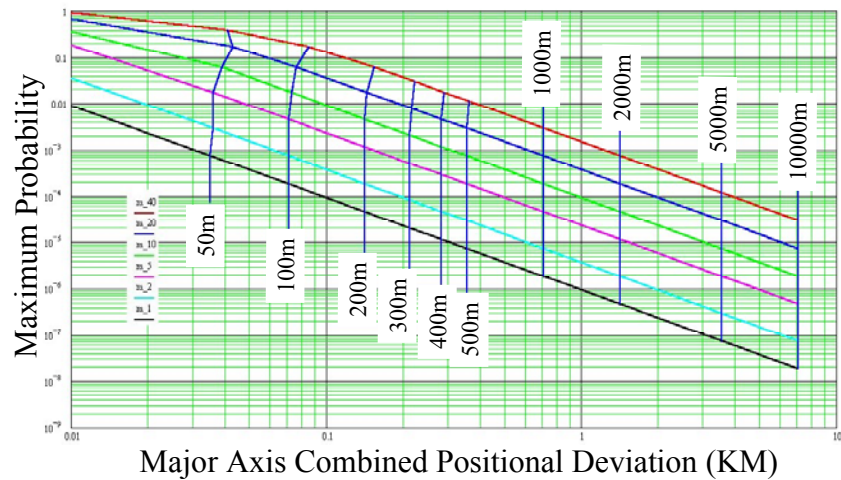


Fig. 7 Maximum Probability Chart for Aspect Ratio of 5

Maximum Probability Analysis (AR = 10)

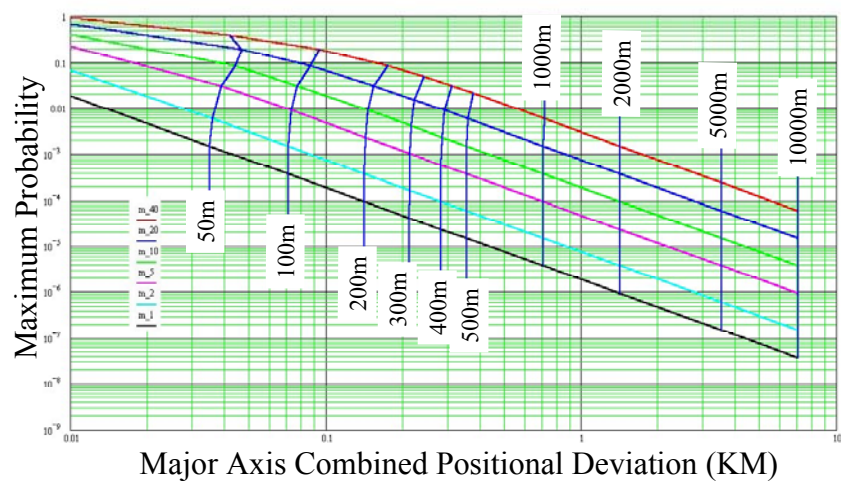


Fig. 8 Maximum Probability Chart for Aspect Ratio of 10

Maximum Probability Analysis (AR = 100)

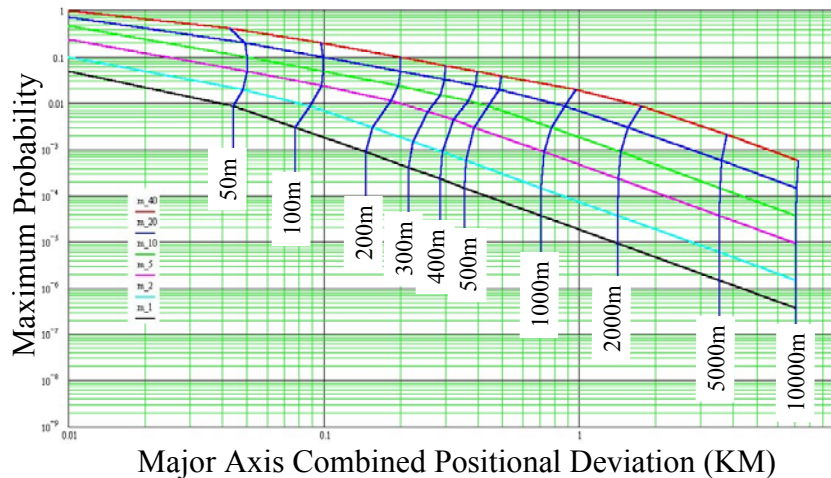


Fig. 9 Maximum Probability Chart for Aspect Ratio of 100

CONCLUSIONS

Charts were created to show the effects of positional uncertainty on orbit conjunction probability calculation. Regions of maximum probability were mapped for various satellite sizes, encounter geometries, and covariance sizes and shapes. Examples were given demonstrating chart use to assess probability dilution, determine ephemeris accuracy requirements, and establish distances for probability-based keepout zones. **If operating in a region where probability is diluted, the user should consider the maximum probability, not just the computed one.**

ACKNOWLEDGEMENTS

This work was done in support of the Joint Astrodynamics Working Group, chaired by Dr. Michael J. Gabor, and the US STRATCOM Director of Analysis, Dr. David Finkleman.

REFERENCES

1. Foster, J. L., Estes, H. S., "A Parametric Analysis of Orbital Debris Collision Probability and Maneuver Rate for Space Vehicles," NASA JSC 25898, August 1992.
2. Khutorovsky, Z. N., Boikov, V., Kamensky, S. Y., "Direct Method for the Analysis of Collision Probability of Artificial Space Objects in LEO: Techniques, Results, and Applications," Proceedings of the First European Conference on Space Debris, ESA SD-01, pp. 491-508, 1993.
3. Carlton-Wipperfurth, K. C., "Analysis of Satellite Collision Probabilities Due to Trajectory and Uncertainties in the Position/Momentum Vectors," Journal of Space Power, Vol. 12, No. 4, 1993.
4. Chan, K. F., "Collision Probability Analyses for Earth Orbiting Satellites," Advances in the Astronautical Sciences, Vol. 96, pp. 1033-1048, 1997.
5. Berend, N., "Estimation of the Probability of Collision Between Two Catalogued Orbiting Objects," Advances in Space Research, Vol. 23, No. 1, pp. 243-247, 1999.
6. Oltrogge, D., and Gist, R., "Collision Vision Situational Awareness for Safe and Reliable Space Operations," 50th International Astronautical Congress, 4-8 Oct 1999/Amsterdam, The Netherlands, IAA-99-IAA.6.6.07
7. Akella, M. R., Alfried, K. T., "Probability of Collision Between Space Objects," Journal of Guidance, Control, and Dynamics, Vol. 23, No. 5, September-October 2000, pp. 769-772.
8. Chan, K. F., "Analytical Expressions for Computing Spacecraft Collision Probabilities," AAS Paper No. 01-119, AAS/AIAA Space Flight Mechanics Meeting, Santa Barbara, California, 11-15 February, 2001.
9. Patera, R. P., "General Method for Calculating Satellite Collision Probability," AIAA Journal of Guidance, Control, and Dynamics, Volume 24, Number 4, July-August 2001, pp. 716-722.
10. Gottlieb, R. G., Sponaugle, S. J., and Gaylor, D. E., "Orbit Determination Accuracy Requirements for Collision Avoidance," AAS/AIAA Space Flight Mechanics Meeting, February 11-15, 2001, Santa Barbara, California, AAS 01-181.